

# Hall sensor-based speed control of a 3-phase permanent-magnet synchronous motor using a field-oriented algorithm

Abidaoun H. Shallal<sup>1</sup>, Saad Abdulmajeed Salman<sup>2</sup>, Ahmad H. Sabry<sup>3</sup>

<sup>1</sup>Department of Communication, College of Engineering, University of Diyala, Baquba, Iraq

<sup>2</sup>Department of Computer, College of Engineering, University of Diyala, Baquba, Iraq

<sup>3</sup>Department of Computer Engineering, Al-Nahrain University, Al Jadriyah Bridge, Baghdad, Iraq

## Article Info

### Article history:

Received Mar 9, 2022

Revised Jun 14, 2022

Accepted Jul 1, 2022

### Keywords:

3-phase PMSM

Auto-tuning

Field-oriented control

PI controller

Speed controller

## ABSTRACT

To achieve optimum torque per amp, we retain the angle of the stator-current-vector with respect to the rotor-flux at 90 degrees, rather than controlling the amplitude of the stator-current-vector. Without or with the load torque, the proportional integral (PI) controller produced better results in the speed control loop. A controller is required to maintain a consistent speed and improve system performance as the load changes. This work develops an auto-tuning PI speed controller for 3-phase permanent-magnet synchronous motors using field oriented algorithm. The 3-phase voltage from the grid is converted to DC through a transformer and a grid-side rectifier. The DC voltage is converted back into AC through a machine-side inverter, which drives the motor with time-varying load. The objective of field oriented control (FOC) in this work is to control the semiconductor switches in the machine-side power inverter to achieve the desired torque and flux. The stator-currents are measured and fed into the flux observer to obtain the direct-quadrature-zero (DQ-axis) current, the rotor magnetizing current, and the angle of the synchronously rotating reference frame. The results show that the motor's speed response has an earlier transient response and a less steady-state inaccuracy after tuning the controllers during acceleration and torque load adjustments.

*This is an open access article under the [CC BY-SA](https://creativecommons.org/licenses/by-sa/4.0/) license.*



## Corresponding Author:

Ahmad H. Sabry

Department of Computer Engineering, Al-Nahrain University

Al Jadriyah Bridge, Baghdad, Iraq

Email: ahs4771384@gmail.com

## 1. INTRODUCTION

High-performance control systems for induction motors (IM), such as field oriented control (FOC), are widely employed in industry and electric vehicle applications. FOC is mathematical modeling for an induction motor to resemble a DC motor. As a result, designing and implementing this system is simple. sliding mode control (SMC) and other robust and stable control methods must be incorporated to ensure their robustness and stability [1]. Because the use of a 3-phase induction motor is becoming more common, research on speed regulation in 3-phase induction motors is being more widely studied [2]. This is due to the increased use of 3-phase induction motors in the industry, particularly in hybrid automobiles [3].

To regulate the torque on any electrical equipment, we must first control the current. Referring to Figure 1, it is possible to divide this method into four distinct stages; i) measuring the current that already flowing in the motor, which may be conducted by a shunt resistor and an analog-to-digital converter (ADC) converter to take a sample of the current reading. ii) Comparing the desired current with the measured current to produce error signals. iii) Amplifying the error signals to produce an adjustment voltage. It is essential to increase the voltage when there is a low current, and it is required to lower the voltage when the current is

high. iv) Directing the corrective voltage to the motor terminals. These four phases make up the process of current-mode control, which the CPU does thousands, if not tens of thousands, of times every second. Understanding these four steps help to understand field oriented control (FOC).

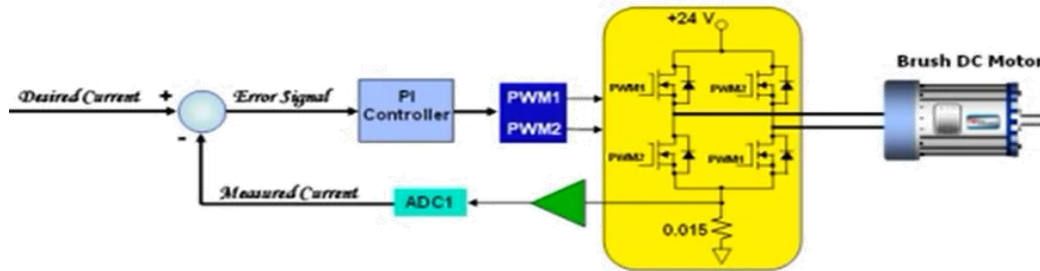


Figure 1. The basic control diagram of a DC motor [4]

For a 3-phase AC machine, there are three currents to control instead of just one. On a space vector diagram, those three currents combine to form a current vector with a specific angle and magnitude. We can generate a current vector with any angle and magnitude by manipulating those 3-phase currents to the exact required values. The question is what is the requested angle in this case? The top value of torque on a given value of current is obtained by plotting the torque created using a permanent magnet 3-phase motor for a current mycophenolate mofetil (MMF) angle and rotor-flux as the torque reaches either + 90 or - 90 degrees, which is also referred to as the maximum Torque per amp angle. Therefore, it is necessary to navigate the MMF vector stator current to be 90 degree related to the rotor flux, which enables the equation of torque (1) to be applied [5]:

$$Torque = \frac{3P}{4} [\lambda_{dr} I_{qs}] \tag{1}$$

Where P and  $\lambda_{dr}$  are constant, and  $I_{qs}$  is adjustable, which means that the 3-phase permanent magnet motor torque is proportional to the product of the component of the stator-current vector at 90 degrees rotor-flux vector. To manage the machine's torque, we keep the angle of the stator-current-vector with respect to the rotor-flux at 90 degrees to achieve maximum torque per amp, rather than regulating the stator-current-vector's amplitude. Therefore, a digital processor is employed to do this process by measuring the rotor-flux angle to calculate the right values for phase A, B, and C currents to generate a stated vector of 90 degrees related to the rotor-flux angle. The voltages are then supplied to the machine's windings in an attempt to regulate the current to the values I just determined. We perform another interrupt after this interrupt service routine and maybe 100 microcircuits later. The rotor has been changed to a different angle by this time, and it is necessary to read that new angle and then compute the present values. This is done in a sequence to illustrate the field-oriented control procedure. It is required to convert the 3-phase current vectors to two orthogonal vectors that provide a current vector of the same net [6]. To put it another way, turn the 3-phase motor into a two-phase motor. Then, instead of having to manage three current values, we simply have to rule two. The forward Clark transition is a term used to describe this process, which is given by (2).

$$\begin{aligned} i_{\alpha} &= \frac{3}{2} i_a \\ i_{\beta} &= \frac{\sqrt{3}}{2} i_b - \frac{\sqrt{3}}{2} i_c \end{aligned} \tag{2}$$

To jump upon the rotating reference frame, whose x-axis is the rotor-flux axis, the following are used (3).

$$\begin{aligned} i_d &= i_{\alpha} \cos \theta_d + i_{\beta} \sin \theta_d \\ i_q &= -i_{\alpha} \sin \theta_d + i_{\beta} \cos \theta_d \end{aligned} \tag{3}$$

The closed-loop speed regulation and field-oriented control (FOC) modeling of a 3-phase permanent magnet synchronous machine (PMSM) powered through the corresponding matrix converter (MC) [7]. To increase the input current quality, the model analyzes a collection of a few input filters of cable influence or supply impedances. A comparison of two kinds of motor speed controllers, namely a proportional/integral (PI), was provided for improving the drive system's performance in both transient and stable settings. In comparison to the PI classic controller, the IP controllers were shown to produce greater performances for motor speed control loops, without or with load torque [8].

An adaptive integral sliding mode manage (SMC) is used as an AC drive system to control the speed of a 3-phase induction motor using field-oriented control [9]. The SMC was used to determine the frequency at which the space vector pulse width modulation (SVPWM) inverter was needed to generate 3-phase electricity. When compared to the classical PI controller, the simulation results of employing the SMC revealed that a good dynamic response may be produced under load disturbances.

The FOC of 3-phase induction motors was regulated utilizing (PI) and (PI) in the study [10]. In this research, the particle swarm optimization (PSO) technique was employed to design I-P controllers that perform better. The two proposed controller systems' operation performances were evaluated in terms of momentary responses, current ripples, and motor torque, to load torque variations. The research [11] compared the performances of indirect field oriented control (IFOC) for controlling the speed of a 3-phase induction motor. The Ziegler-Nichols approach was used to tune the PI controller. The IFOC technique was used in the study [12] to improve indirect field-oriented control (IFOC) to increase the efficiency and performance of 3-phase induction motor (TIM) drives' variable speed control. To improve the variable speed control of IFOC in TIM, a technique based on the PSO algorithm was developed. All of the tests confirmed the controller's speed response resilience under various mechanical stress and speed situations. The research [13] discussed an adaptive fuzzy logic control (AFLC) technique for TIM to provide robustness and quick dynamic responses for low and high-speed variations, as well as good torque and efficiency. The AFLC and PI based on the levenberg marquart (LM) approach were simulated, examined, and developed for the indirect FOC (IFOC) LM drive system. The results showed that the ALFC based on LM gives the IFOC IM drive system better, more effective, and faster reactions, with reduced overshoot, rise, and settling time. Induction motors have some drawbacks, one of which is the non-linear characteristics of non-linear parameters, particularly rotor resistance, which varies depending on operating conditions, causing it to lose speed if the load changes. Of course, this has an impact on the performance of an induction motor. A controller is required to maintain a consistent speed and improve system performance as the load changes. The FOC approach with the PI controller to describe direct-quadrature parameters (D-Q) was used by [3].

A position and speed controls of PMSM using a genetic algorithm controller and hall effect sensors were performed by [14]. The results obtained from this study reveal that the proposed control system was effective, reliable, and robust. Many industrial variable speed applications [15] and [16] necessitate speed and position control. However, the PMSMs' performances are extremely sensitive to changes in parameters and load. To address these issues, numerous current control strategies for speed control have been presented, including PI or proportional-integral-derivative (PID) control, fuzzy logic control [17], genetic algorithm [18], and neural network control approaches [19], [20]. In PMSMs, determining the rotor position and performing commutation at the exact time is critical. The information on location and speed is received through the rotor using Hall Effect sensors and encoders. Although position and speed data can be obtained without the use of sensors, the microprocessor must have a large memory capacity and a fast processing speed. Sensors with higher resolution, such as optical encoders or resolvers, are usually required for applying sinusoidal commutation to such a motor [21]. These sensors, however, are expensive and cannot be used for low-cost operations. The hall effect sensors in PMSM also discussed by [22]. The proposed approach for sinusoidal commutation applies sine PWM pulses for inverter switching based on rotor position information provided by Hall sensors. In this method, the modulation index is altered using a PI controller for PMSM speed control. Using a texas instruments (TI) digital signal processor (DSP) TMS320F2812 [23], the method was successfully tested on a 400W PMSM motor configuration. The results revealed that using FOC can improve the output response while also reducing the time it takes to achieve the reference value.

## 2. METHOD

For 3-phase induction motors, a stator-current in the stator windings creates a magnetic field that rotates at a single speed causing the rotor to move at a slightly slower speed, which is necessary for torque production [24]. In field oriented control, the motor torque and the motor flux are controlled independently. This requires that the three sinusoidal stator-currents are first converted into a DC component on a synchronized rotary reference frame using Clark and Park formation [25]. By turning the time domain components of a 3-phase system into *abc* frame components in a stationary alpha beta 0 reference frame or a revolving dq0 reference frame attached to the rotor, mathematical transformations define the most fundamental notion in field-oriented management of AC machines. It is also possible to utilize the inverse transform to travel from *dq* to alpha-beta and then back to *abc* frame, but knowing the rotor location is required; otherwise, the values in the rotor reference frame cannot be obtained. Figure 2 shows the 3-phase current representation and the *abc-dq* axis frame representation.

The D-axis current of the new frame allows controlling the rotor flux and provides a way to adjust the motor frequency and power factor. The gate driver is implemented using the six poles gate multiplexer as

an interface between the controller and the plant. As in any physical system, some sensors are used to measure the relevant signals such as currents and voltages. The mechanical part and the mechanical load are represented by a machine inertia block and the torque source, which allows adjusting the load torque in the system. The design of the controller is done by using field-oriented control based on PI controllers including the inverse parke transform, and the PWM generation. The Q-axis control is orthogonal on the D-axis and allows controlling of the motor torque. In this work, the model under consideration can be shown in Figure 3.

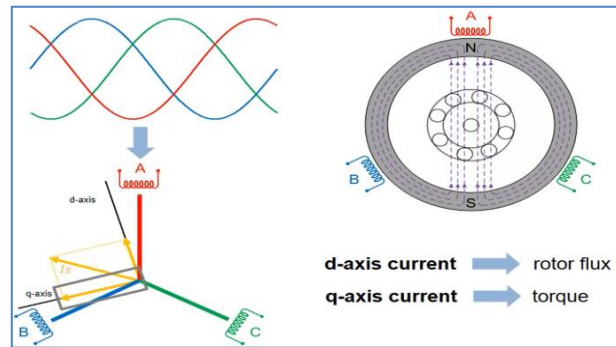


Figure 2. The 3-phase current representation and the *abc-dq* axis frames representation

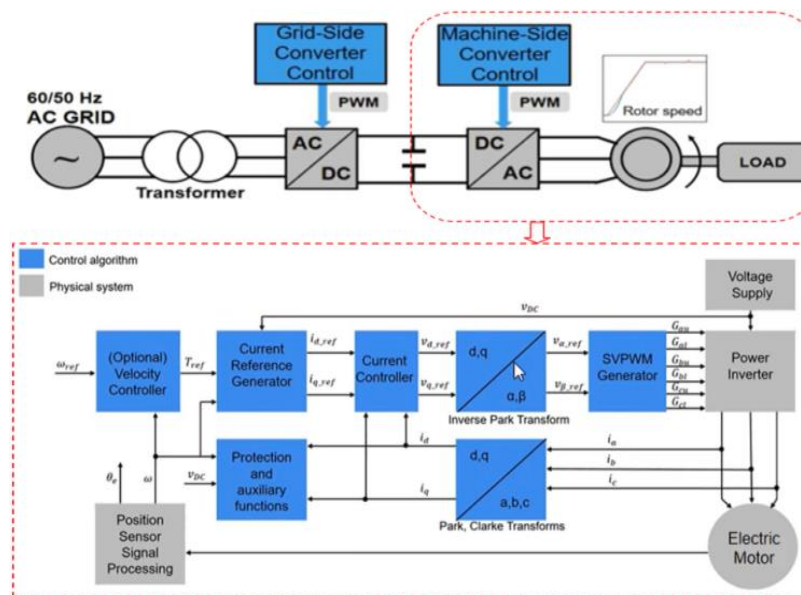


Figure 3. The considered model and the developed control algorithm

In this model, the 3-phase voltage from the grid is converted to DC through a transformer and a grid-side rectifier. The DC voltage is converted back into AC through a machine-side inverter, which drives an induction motor with time-varying load. The objective of FOC in this work is to control the semiconductor switches in the machine-side power inverter to achieve the desired torque and flux. The control loops contain four PI controllers. The stator-currents are measured and fed into the flux observer to obtain the direct-quadrature-zero (DQ-axis) current, the rotor magnetizing current, and the angle of the synchronously rotating reference frame. The rotating frame angle is used at a later stage to perform inverse Clarke and Park transformation. The machine-side of the converter control is shown in Figure 4, where the original plant PID-controller is shown in Figure 4(a), and the PID-controller with adding Auto-tuner block is shown in Figure 4(b).

Figure 5 demonstrates the controller of the grid stage converter. The measured rotor speed, magnetizing current, and the provided references are used by the flux and the rotor speed controllers in the outer loop to calculate references for the DQ-axis currents. Based on these, the current controllers in the inner control loop determine the required stator voltage in DQ-frame. After applying inverse Park and Clarke transformations, the required stator voltage is used by a PWM generator to generate the control signals for the semiconductor switches in the machine side inverter.

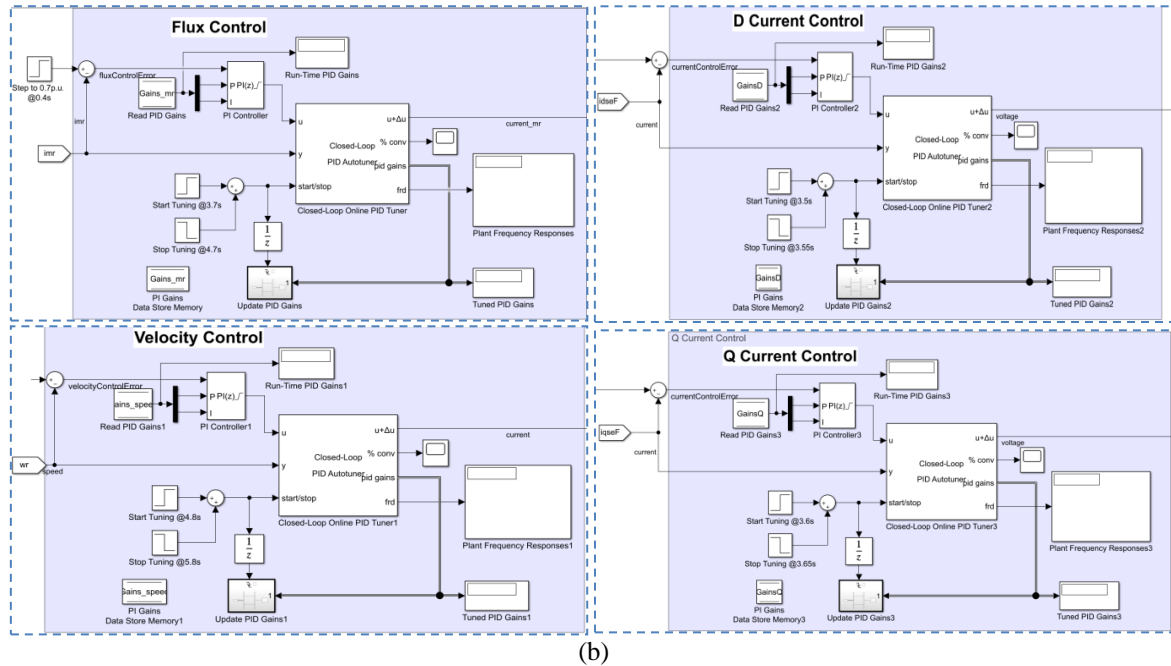
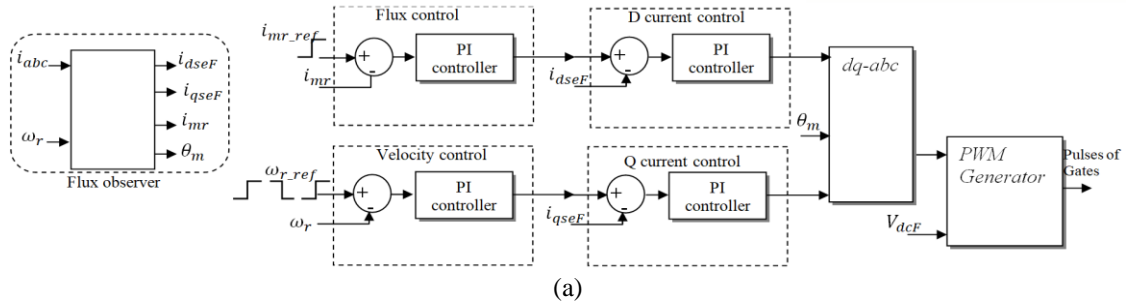


Figure 4. Machine side converter control; (a) original plant PID-controller and (b) adding auto-tuner block

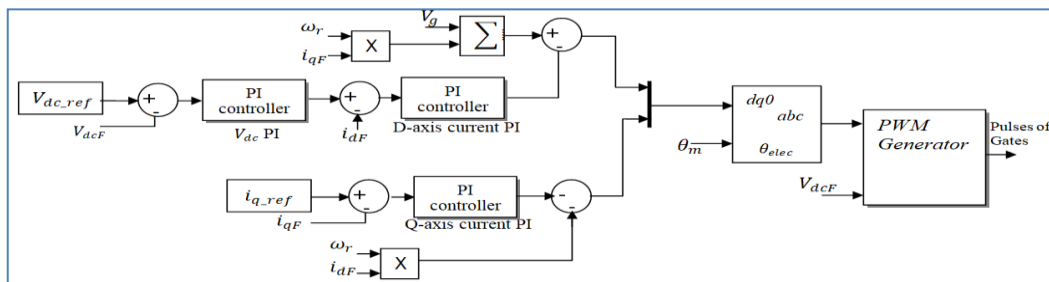


Figure 5. Grid-side converter control

Closed-loop tuning has the advantage of keeping the plant close to its normal operating point while maintaining safe operation during the tuning process. The inputs of the closed-loop online PID autotuner include the plant output, the PI controller output, and the time window when the tune happens. The outputs include the tuned PID gains and the estimated frequency response. The flowchart shown in Figure 6 provides a general overview of the PID auto-tuning method.

Because the tuning is allowed for one controller at a time, we place the PI block after all 4 controllers to be able to tune them in a single simulation. The PI controller will be tuned sequentially with between  $t = 3.5$  seconds and  $t = 5.8$  seconds starting with the D-axis current loop and followed by the Q-axis current loop, the rotor-flux loop, and finally the rotor speed loop. We set the appropriate values to the target bandwidth and target phase margin as a block configuration. We also specify the amplitude of the excitation signal in the experiment to 0.01. The rotating frame angle is used at a later stage to perform inverse Clarke and Park transformation.

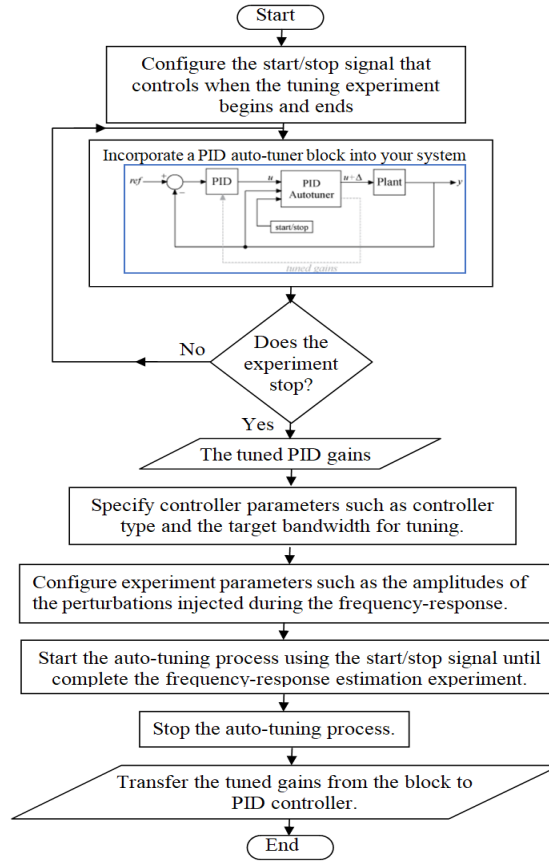


Figure 6. The flowchart provides a general overview of the PID auto-tuning method

### 3. RESULTS AND DISCUSSION

For the simulation, the gains in the PI blocks are set at initial values. The measurements of the magnetizing stator-current, comparison of the torques of the motor with the required load torque, and the rotor speed before tuning compared with reference are shown in Figure 7. On the grid-side, the waveforms of each grid voltage, current, DC-link voltage, and the active power delivered by the grid are shown in Figure 8.

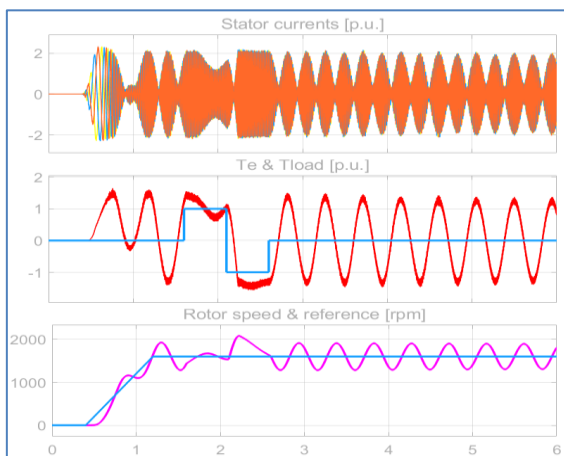


Figure 7. (1) The magnetizing stator-current, (2) comparison of the torques of the motor with the required load torque, and (3) the rotor speed before tuning compared with the reference

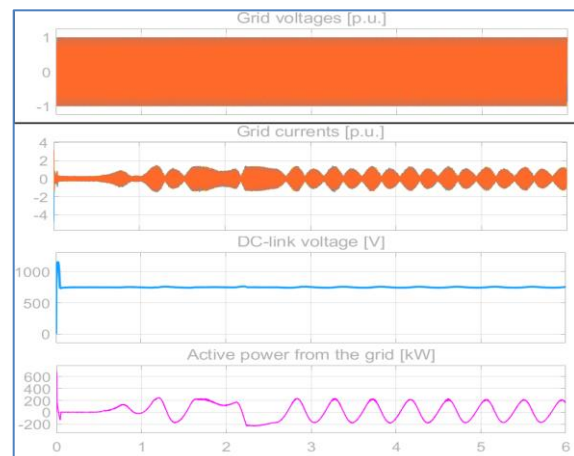


Figure 8. Grid-side waveforms of grid voltage, current, DC-link voltage, and the active power delivered by the grid

The results indicate that the initial PI gains do not provide the best performance and the response is under-damped with significant overshoot. To get better reference performance, we tune the PI gains by using a closed-loop PID Auto-Tune block. This block injects an excitation signal during closed-loop operation to estimate the plant frequency response and uses this estimate to automatically tune PID gains. After running the model, we can see that before the tuning begins the response is identical to the original model. The four controllers were tuned separately in the FOC model since the autotuner of the closed-loop PID only adjusts a single PI controller at a time. Following the timing in Table 1, we tuned the controllers of the inner-loop first, then that for the outerloop.

The data store memory block is used to update the controller gains after each PI controller has been tuned. MATLAB/Simulink is used to create the FOC model. In one simulation, all four controllers are tuned. Furthermore, speed dynamics are examined after and before the controllers are tuned. Scenarios of these experiments include the torque load changes (magnitude of 1 p.u.) and acceleration process. The current and speed responses during tuning are shown in gray in the previous figure, ranging from 3.51 to 5.81 seconds. The changes in motor speed and current are very low. The speed of the motor approaches a nominal value of (1600) rpm before the auto-tuning process starts. The gain values of the four PI controllers before and after the tuning process are listed in Table 2.

The measurements of the magnetizing stator-current, comparison of the torques of the motor with the required load torque, and the rotor speed before tuning compared with reference are shown in Figure 9. On the grid-side, the waveforms of each grid voltage, current, DC-link voltage, and the active power delivered by the grid are shown in Figure 10. The tune gains will be saved and updated once the tuning is finished. These gain values are used to create fresh values from which the auto-tuning blocks can be deleted. Before and after the auto-tuning process, the same torque loads and rotor speed references are used. Figure 11 shows the plot of rotor speed errors against the nominal (1,600) rpm after and before tuning the controllers with the Auto-tuner PID closed-loop function. In order to compare controllers' performance side-by-side, the error curves of the speed were aligned in time. The asynchronous motor's speed response has an earlier transient response and a less steady-state inaccuracy after tuning the controllers during acceleration and torque load adjustments.

Table 1. Timing table of the controllers' tuning intervals

| Timing interval              | Description                                      |
|------------------------------|--|
| $3.51 \geq t_{id} \geq 3.55$ | The time tuning of the current controller d-axis |
| $3.6 \geq t_{iq} \geq 3.65$  | The time tuning of the current controller q-axis |
| $3.7 \geq t_f \geq 4.7$      | The time tuning of the flux controller           |
| $4.8 \geq t_w \geq 5.81$     | The time tuning of the speed controller          |

Table 2. The gain values of the four PI controllers before and after the tuning process

| Description          | Gains before tuning |         | Gains after tuning |       |
|----------------------|---------------------|---------|--------------------|-------|
|                      | $K_p$               | $K_i$   | $K_p$              | $K_i$ |
| D-axis PI controller | 1.08                | 207.58  | 1.611              | 627.6 |
| Q-axis PI controller | 1.08                | 210.02  | 2.029              | 829.9 |
| Flux PI controller   | 52.22               | 2790.51 | 129.3              | 1732  |
| Speed PI controller  | 65.47               | 3134.24 | 158.8              | 2110  |

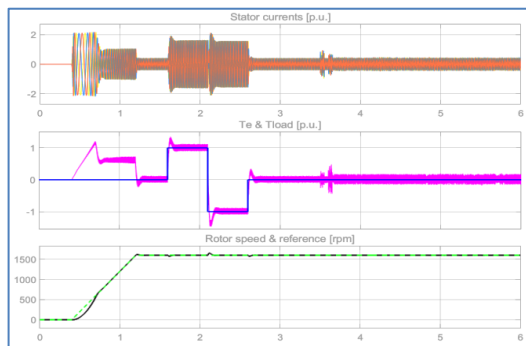


Figure 9. The measurements after tuning the gains of the PI controllers of (1) The magnetizing stator-current, (2) comparison of the torques of the motor with the required load torque, and (3) the rotor speed before tuning compared with the reference

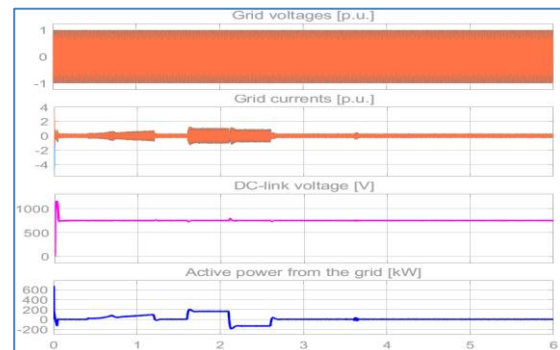


Figure 10. The measurements after tuning the gains of the PI controllers of grid-side waveforms of grid voltage, current, DC-link voltage, and the active power delivered by the grid

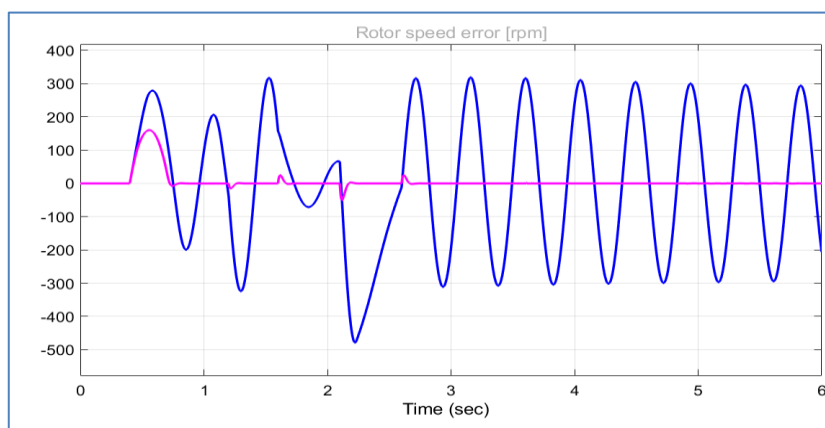


Figure 11. The error waveforms of the rotor speed before and after the tuning

#### 4. CONCLUSION

The tuning technique seeks to achieve the phase margin and control bandwidth we specify while balancing resilience and performance. We can set up logic to send the tuned gains from the tuner to the PID controller in real-time, allowing us to test closed-loop performance. The obtained results indicate that the initial PI gains do not provide acceptable performance and the response was under-damped with significant overshoot. To get better reference performance, we tuned the PI gains by using a closed-loop PID Auto-Tune block, which injects an excitation signal during closed-loop operation to estimate the plant frequency response and using these estimated values to automatically tune PID gains. The results also show that the asynchronous motor's speed response has earlier transient responses and a less steady-state inaccuracy after tuning the controllers during acceleration and torque load adjustments.

#### REFERENCES





- [1] D. C. Happyanto, A. W. Aditya, and B. Sumantri, "Boundary-layer effect in robust sliding mode control for indirect field oriented control of 3-phase induction motor," *Int. J. Electr. Eng. Informatics*, 2020, doi: 10.15676/ijeei.2020.12.2.2.
- [2] A. H. Shallal, A. F. Nashee, and A. E. Abbas, "Smart actuator for IM speed control with F28335 DSP application," *Indones. J. Electr. Eng. Comput. Sci.*, 2021, doi: 10.11591/ijeecs.v24.i3.pp1421-1431.
- [3] R. Fauzi and J. Khair, "Pemodelan direct quadrate (D-Q) on the speed control of a three-phase induction motor with (In Bahasa: pada kendali kecepatan motor induksi tiga fasa dengan) field oriented control (FOC) control based (In Bahasa: berbasis kendali) P-I," *Sci. Comput. Sci. Informatics J.*, 2019, doi: 10.22487/j26204118.2018.v1.i2.12059.
- [4] A. Mazaheri and A. Radan, "Performance evaluation of nonlinear Kalman filtering techniques in low speed brushless DC motors driven sensor-less positioning systems," *Control Eng. Pract.*, 2017, doi: 10.1016/j.conengprac.2017.01.004.
- [5] I. Boldea, J. Zhang, and S. A. Nasar, "Low-speed flux-reversal machines: Pole-face versus inset PM stators," *Electr. Power Components Syst.*, 2003, doi: 10.1080/15325000390219811.
- [6] S. S. Kaushilk, M. A. Khan, T. A. Khan, and P. R. Sharma, "Comparison of performance of vector control induction motor supplied by zsi with and without pi controller," *Int. J. Sci. Technol. Res.*, 2020.
- [7] M. Bouazdia, M. Bouhamida, R. Taleb, and M. Denai, "Performance comparison of field oriented control based permanent magnet synchronous motor fed by matrix converter using PI and IP speed controllers," *Indones. J. Electr. Eng. Comput. Sci.*, 2020, doi: 10.11591/ijeecs.v19.i3.pp1156-1168.
- [8] Iswanto, A. Ma'arif, R. D. Puriyanto, N. M. Raharja, and S. N. Rahmadhia, "Arduino embedded control system of DC motor using proportional integral derivative," *Int. J. Control Autom.*, 2020.
- [9] F. R. Yasien and W. H. Nasser, "Speed controller of three phase induction motor using sliding mode controller," *J. Eng.*, 2019, doi: 10.31026/j.eng.2019.07.07.
- [10] F. H. Faris, A. T. Humod, and M. N. Abdullah, "A comparative study of PI and IP controllers for field oriented control of three phase induction motor," *Iraqi J. Comput. Commun. Control Syst. Eng.*, 2019, doi: 10.33103/uot.ijccce.19.2.7.
- [11] H. Aziri, F. A. Patakor, M. Sulaiman, and Z. Salleh, "Comparison performances of indirect field oriented control for three-phase induction motor drives," *Int. J. Power Electron. Drive Syst.*, 2017, doi: 10.11591/ijpeds.v8i4.pp1682-1692.
- [12] J. Abd Ali, M. A. Hannan, and A. Mohamed, "Improved indirect field-oriented control of induction motor drive based PSO algorithm," *J. Teknol.*, 2016, doi: 10.11113/jt.v78.8888.
- [13] K. Zeb et al., "Adaptive fuzzy logic controller for indirect field oriented controlled induction motor," in *2019 2nd International Conference on Computing, Mathematics and Engineering Technologies, iCoMET 2019*, 2019, doi: 10.1109/ICOMET.2019.8673498.
- [14] E. Bekiroglu and A. Dalkin, "Comparison of trapezoidal and sinusoidal pwm techniques for speed and position control of pmsm," *Adv. Electr. Electron. Eng.*, 2020, doi: 10.15598/aece.v18i4.3842.
- [15] Y. Lee and J. I. Ha, "High efficiency dual inverter drives for a PMSM considering field weakening region," in *Conference Proceedings - 2012 IEEE 7th International Power Electronics and Motion Control Conference - ECCE Asia, IPEMC 2012*, 2012, doi: 10.1109/IPEMC.2012.6258939.
- [16] C. Elmas, O. Ustun, and H. H. Sayan, "A neuro-fuzzy controller for speed control of a permanent magnet synchronous motor drive," *Expert Syst. Appl.*, 2008, doi: 10.1016/j.eswa.2006.10.002.







- [17] N. P. Ananthamoorthy and K. B. Baskaran, "High performance hybrid fuzzy PID controller for permanent magnet synchronous motor drive with minimum rule base," *JVC/Journal Vib. Control*, 2015, doi: 10.1177/1077546313484349.
- [18] R. K. Jatoth and A. Rajasekhar, "Speed control of PMSM by hybrid genetic artificial bee colony algorithm," in *2010 IEEE International Conference on Communication Control and Computing Technologies, ICCCCCT*, 2010, doi: 10.1109/ICCCCT.2010.5670559.
- [19] C. Elmas and O. Ustun, "A hybrid controller for the speed control of a permanent magnet synchronous motor drive," *Control Eng. Pract.*, 2008, doi: 10.1016/j.conengprac.2007.04.016.
- [20] Y. Ahmed, A. Hoballah, E. Hendawi, S. Al Otaibi, S. K. Elsayed, and N. I. Elkalashy, "Fractional order pid controller adaptation for pmsm drive using hybrid grey wolf optimization," *Int. J. Power Electron. Drive Syst.*, 2021, doi: 10.11591/ijpeds.v12.i2.pp745-756.
- [21] M. N. S. Hakim and S. Riyadi, "The use of input capture method to increase torque on switched reluctance motor," in *Journal of Physics: Conference Series*, 2020, doi: 10.1088/1742-6596/1444/1/012014.
- [22] A. H. Sabry and P. J. Ker, "DC environment for a refrigerator with variable speed compressor; power consumption profile and performance comparison," *IEEE Access*, 2020, doi: 10.1109/ACCESS.2020.3015579.
- [23] L. Guo, "Implementation of digital PID controllers for DC-DC converters using digital signal processors," in *2007 IEEE International Conference on Electro/Information Technology, EIT 2007*, 2007, doi: 10.1109/EIT.2007.4374445.
- [24] D. R. E. Trejo, D. U. C. Delgado, G. Bossio, E. Bárcenas, J. E. H. Díez, and L. F. L. Cordero, "Fault diagnosis scheme for open-circuit faults in field-oriented control induction motor drives," *IET Power Electron.*, 2013, doi: 10.1049/iet-pel.2012.0256.
- [25] I. Calomfirescu, "The simulation of an induction motor in transient behavior taking into account the saturation effect," in *2012 International Conference on Applied and Theoretical Electricity, ICATE 2012 - Proceedings*, 2012, doi: 10.1109/ICATE.2012.6403421.

## BIOGRAPHIES OF AUTHORS







**Abidaoun H. Shallal**     Born in Diyala, Iraq. He received a Bachelor's and Master's degree in Electrical and Electronic Engineering from Al-Rasheed College of Engineering and Science, University of Technology, Iraq, 1992 and 2001, respectively, and Ph.D. in electrical and electronic engineering, Control engineering from Altinbas University, Istanbul, Turkey in 2019. He taught many subjects in his field of expertise. He has a lot of research publications in international journals, his research interests are in the field of control and robots. He can be contacted at email: abidaoun.hamdan@gmail.com.



**Saad Abdulmajeed Salman**     was born in Diyala, Iraq. He received a B.Sc. Degree in electrical and electronic engineering, master's degree in electrical and electronic engineering, and Ph. Degree in electrical and electronic engineering from the University of Technology, Al-Rashied College of engineering & science, Baghdad, Iraq, in 1992, 1997, and 2006, respectively. He was working as the head of the computer engineering department college of engineering-Diyala university-Iraq from 2004 to 2012. His current research interests include *Control Systems* and applications. He has worked in various colleges, including: from 1992 to 2004, working as a lecturer at the university of technology, Al-Rashied college of engineering & science, Baghdad, Iraq. From 1997 to 2000 working as an external lecturer in the technical institute of Baquba, the electrical department. From 1999 to 2004 working as an external lecturer at Diyala University, college of engineering, electronic department. From 2004 to 2022 working as a Lecturer at Diyala university, college of engineering, computer engineering department. He can be contacted at email: drsaad\_eng@uodiyala.edu.iq.



**Ahmad H. Sabry**     was born in Baghdad, Iraq. He received his B.Sc. and M.Sc. degrees in electrical and electronics, control and automation, and engineering from the University of Technology-Baghdad, Iraq, in 1994 and 2001, respectively. He received a Ph.D. degree in DC-Based PV-Powered Home Energy System from the Department of Electrical and Electronic Engineering, control, and automation at UPM, Malaysia in 2017. He is the author of more than 35 articles, and more than 5 inventions, and holds one patent. His research interests include integrated solar powered smart home system based on voltage matching, DC distribution, industrial robotic systems, and wireless energy management systems. He is a reviewer in more than three ISI journals. He is currently a post-doctorate researcher at Universiti Tenaga Nasional (UNITEN). He can be contacted at email: ahs4771384@gmail.com.